

Electron paramagnetic resonance investigation of the ferroelastic phase transition in the  $K_3Na(SeO_4)_2$  single crystal

This article has been downloaded from IOPscience. Please scroll down to see the full text article.

2002 J. Phys.: Condens. Matter 14 8121

(<http://iopscience.iop.org/0953-8984/14/34/330>)

View [the table of contents for this issue](#), or go to the [journal homepage](#) for more

Download details:

IP Address: 171.66.16.96

The article was downloaded on 18/05/2010 at 12:28

Please note that [terms and conditions apply](#).

# Electron paramagnetic resonance investigation of the ferroelastic phase transition in the $\text{K}_3\text{Na}(\text{SeO}_4)_2$ single crystal

S Jerzak<sup>1</sup> and B Mroz<sup>2</sup>

<sup>1</sup> Department of Physics and Astronomy, York University, 4700 Keele St., Toronto, Canada M3J 1P3

<sup>2</sup> Faculty of Physics, Adam Mickiewicz University, Umultowska 85, 61-614 Poznan, Poland

Received 13 February 2002

Published 15 August 2002

Online at [stacks.iop.org/JPhysCM/14/8121](http://stacks.iop.org/JPhysCM/14/8121)

## Abstract

Electron paramagnetic resonance (EPR) of  $\text{SeO}_3^-$  radicals in  $\text{K}_3\text{Na}(\text{SeO}_4)_2$  single crystal is reported. Two  $\text{SeO}_3^-$  radicals of the same orientation but different hyperfine parameters were used as paramagnetic probes to study the ferroelastic phase transition. A gradual change of orientation of the Se–O(1) bond in the  $bc$ -plane is observed below 329 K. At room temperature, the Se–O(1) bond is deflected by  $3^\circ$  from the  $c$ -axis in the  $bc$ -plane. Narrowing of EPR lines above 329 K is associated with an ordering process of the Se–O(1) bonds. The temperature hysteresis indicates the first-order phase transition at 329 K.

## 1. Introduction

$\text{K}_3\text{Na}(\text{SeO}_4)_2$  (KNSe) is a member of the glaserite subfamily of isostructural crystals with the general formula  $\text{K}_3\text{Na}(\text{XO}_4)_2$ , where  $X = \text{S}, \text{Se}, \text{Cr}, \text{Mo}$ . Three members of this group are ferroelastic:  $\text{K}_3\text{Na}(\text{MoO}_4)_2$  below 513 K [1], KNSe below 334 K [2] and  $\text{K}_3\text{Na}(\text{CrO}_4)_2$  below 239 K [3]. Ferroelasticity in  $\text{K}_3\text{Na}(\text{SO}_4)_2$  has not been observed yet.

The ferroelastic phase transition in KNSe takes place through an intermediate temperature phase (ITP) between  $T_0 = 346$  K and  $T_c = 334$  K. The ITP symmetry was reported to be  $32$  or  $3$  [4] and  $2 m^{-1}$  [5]. Three ferroelastic domains are present below 334 K. Domains become dimmed, gradually fade away above 334 K and are dependent on the thermal history of the sample [5]. The ITP was reported to be optically uniaxial by some authors [5] and biaxial by others [4]. The molecular mechanism of the phase transition is not fully understood. X-ray diffraction investigation conducted at 291 and 390 K shows that the phase transition is accompanied by the shift of two inequivalent potassium cations K(1) and K(2) as well as shift and tilting of  $\text{SeO}_4^{2-}$  anions by  $7.6^\circ$  [6]. On the basis of Raman studies [7], it was concluded that the ferroelastic phase transition is associated with librational motion of tetrahedral anions  $\text{SeO}_4^{2-}$ . The ordering process of these anions takes place in two stages: at 346 K the Se–O(1) bonds start to deviate from the  $c$ -axis. This process is manifested in the Raman spectra

by a gradual increase of the intensity of the band of lattice vibrations at  $60\text{ cm}^{-1}$ . The phase transition at 334 K was explained by hindered rotations of the anions  $\text{SeO}_4^{2-}$  about the Se–O(1) bond, which is along the threefold symmetry axis above 346 K. This process was associated with Raman bands at 36 and  $28\text{ cm}^{-1}$  at 80 K. It was suggested that only two mutually perpendicular domains exist in the ITP, the two domains being related to the deviation of the Se–O(1) bond along two perpendicular directions [8].

Various experimental techniques were used to study the phase transitions in KNSe. Macroscopic measurements such as low-frequency dielectric, adiabatic calorimetry, thermal expansion and linear birefringence ones detect the main anomaly at  $T_0 = 346\text{ K}$  [2, 5], while techniques such as the Raman [7] and Brillouin [8] scattering methods detect it at  $T_c = 334\text{ K}$ . The phase transition at 346 K is of the second-order (continuous) type, while the phase transition at 334 K is of the first-order (discontinuous) type.

The ferroelastic phase transition in KNSe is classified as an improper one. This is supported by observation of the doubling of the unit cell along the  $c$ -axis [6] and different behaviours of the anomalies of the elastic coefficients:  $c_{66}$  shows an anomaly at  $T_c = 334\text{ K}$ ,  $c_{33}$  at  $T_0 = 346\text{ K}$  and  $c_{44}$  at both  $T_c = 334\text{ K}$  and  $T_0 = 346\text{ K}$  [8].

## 2. Experimental procedure

Single crystals of KNSe were grown isothermally from a saturated aqueous solution of the product of synthesis of chemically pure sodium, potassium hydroxide and selenate acid at 315 K. The synthesized compound was purified by recrystallization from distilled water. Excellent quality, colourless and transparent crystals were obtained in the form of a hexagonal prism. The composition of the crystal was confirmed by atomic emission spectroscopy.

Pseudo-hexagonal twins and ferroelastic domains are visible in polarized light when observed along the  $c$ -axis. Samples for electron paramagnetic resonance (EPR) measurements were ferroelastically monodomain, irradiated at room temperature with  $\text{Co}^{60}$   $\gamma$ -rays with a dose of  $1.3 \times 10^6$  rad to create paramagnetic free radicals. Upon irradiation, crystals turned light brown. The EPR spectra were recorded on a BRUKER X-band spectrometer. The sample temperature was changed by gently blowing nitrogen gas, passing through the temperature controller.

## 3. Experimental results and discussion

The spectrum recorded at room temperature with the magnetic field parallel to the crystallographic  $a$ -axis is shown in figure 1. Various paramagnetic radicals are created by  $\gamma$ -irradiation. EPR lines designated as  $A_1$  and  $A_2$  were unambiguously identified as associated with  $\text{SeO}_3^-$  radicals and lines designated as B as associated with  $\text{SeO}_4^{3-}$  radicals. Other radicals such as  $\text{SeO}_2^-$ ,  $\text{SeO}_4^-$  are probably present as well but were not analysed. Each radical possesses one unpaired electron ( $S = 1/2$ ) and their spectrum consists of central lines due to isotopes  $^{74}\text{Se}$  (abundance 0.87%),  $^{76}\text{Se}$  (abundance 9.02%),  $^{78}\text{Se}$  (abundance 23.52%),  $^{80}\text{Se}$  (abundance 49.82%) and  $^{82}\text{Se}$  (abundance 9.19%), all with the nuclear spin  $I = 0$ , and a very weak hyperfine doublet due to the isotope  $^{77}\text{Se}$  with nuclear spin  $I = 1/2$  (abundance 7.58%).

For freshly irradiated crystals, the EPR lines due to the radical  $A_1$  are stronger than those due to the radical  $A_2$ , but after about a couple of weeks the radical  $A_1$  decays, while  $A_2$  becomes stronger. The decay process of radical  $A_1$  is accelerated dramatically at higher temperature and it cannot be observed above approximately 380 K. Figure 2 shows the change of the intensity of the two radicals upon heat treatment of the crystal and about two weeks after the irradiation.

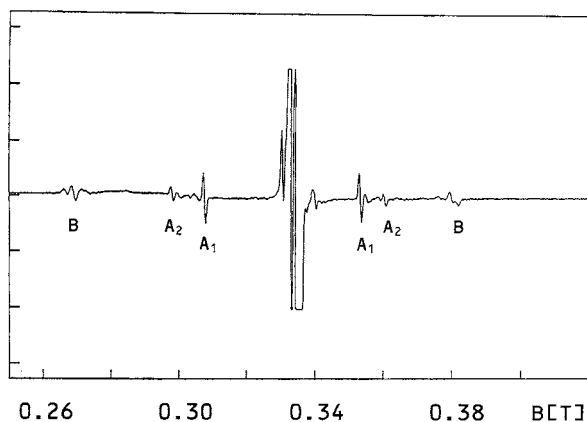


**Figure 1.** The EPR spectrum recorded in the  $ac$ -plane. Symbols  $A_1$  and  $A_2$  represent radicals  $SeO_3^-$  and  $B$  represents the radical  $SeO_4^{3-}$ . Strong EPR lines at the centre are due to Se isotopes with nuclear spin  $I = 0$ .

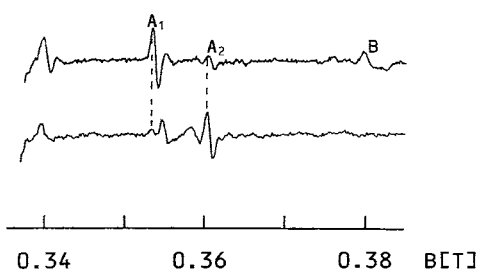


**Figure 2.** Change of the intensity of the EPR lines for radicals  $A_1$  and  $A_2$  upon heat treatment at 360 K and two weeks after irradiation.  $A_1$  disappears and  $A_2$  becomes stronger.

The two  $SeO_3^-$  radicals  $A_1$  and  $A_2$  have the same orientation, as verified by the angular dependence in the three crystallographic planes (figure 3), but differ in intensity and hyperfine structure parameters. These radicals are formed by loss of one oxygen and an electron capture. The  $SeO_3^-$  radical has  $C_{3v}$  symmetry. Its ground state is a molecular orbital of  $^2A_1$  symmetry made up primarily of a  $p_z$  atomic orbital of the Se atom, which is parallel to the axis of highest symmetry of the radical. The largest hyperfine splitting occurs for the magnetic field parallel to this symmetry axis [9, 10].

The tensors  $\mathbf{g}$  and  $\mathbf{T}$  for  $SeO_3^-$  radicals are both axially symmetric as indicated by angular variation of the EPR lines in the  $ab$ -plane (figure 3). The symmetry axis is perpendicular to the plane of three oxygens and along the axis connecting the Se atom to the vacant oxygen site. According to x-ray diffraction study [6], this direction corresponds to the Se–O(1) bond very accurately. This bond must be the weakest of the four Se–O bonds, because radicals with the symmetry axis corresponding to Se–O(2–4) bonds are either not present or very weak and difficult to analyse. According to x-ray diffraction study, the Se–O(1) bond is the shortest of the four Se–O bonds in the  $SeO_4^{2-}$  anion. This does not mean that the bond is strongest. The shortest bond length was accounted for by a ‘riding motion’ correction due to movement of the oxygen [6].

The experimental data can be described by spin Hamiltonian  $H = \beta S\mathbf{g}B + STI$ . The first term is electronic Zeeman term and the second term is the Se hyperfine term. The principal values of the tensors  $\mathbf{g}$  and  $\mathbf{T}$  as well as the isotropic part of the hyperfine interaction  $T_{iso}$  for radicals  $A_1$  and  $A_2$  in the paraelastic phase ( $T = 355$  K) are given in table 1.

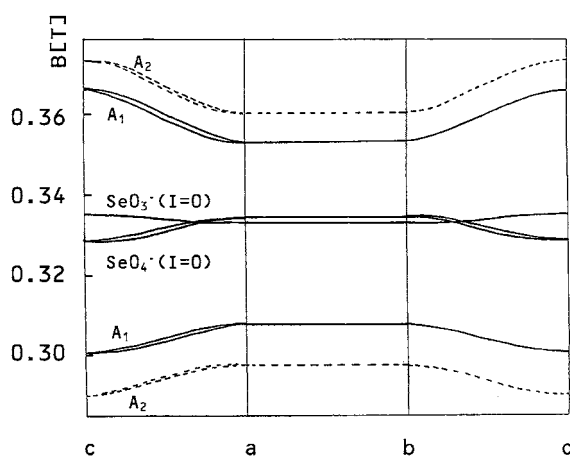


**Figure 3.** Angular variation of the resonance lines due to radicals A<sub>1</sub> (solid curve) and A<sub>2</sub> (broken curve) in three planes: *ab*, *ac* and *bc*. The angular variation of three strong lines at the centre of the spectrum is shown as well. Two nonequivalent but symmetry-related centres are observed in the *bc*-plane. In the *ac*-plane only one centre is observed for both A<sub>1</sub> and A<sub>2</sub>.

**Table 1.** Principal values of the tensors **g** and **T** and direction cosines of their principal *z*-axis in the *a*, *b*, *c*-axes system for radicals A<sub>1</sub> and A<sub>2</sub> at *T* = 355 K. Both tensors are axially symmetric in the paraelastic phase.

Radical	<b>g</b>	<b>T</b> (mT)	Direction cosines
A <sub>1</sub>	$g_{\parallel} = 2.004$	$T_{\parallel} = 64.8$	(001)
	$g_{\perp} = 2.015$	$T_{\perp} = 45.8$	
		$T_{iso} = 52.1$	
A <sub>2</sub>	$g_{\parallel} = 2.004$	$T_{\parallel} = 82.9$	(001)
	$g_{\perp} = 2.015$	$T_{\perp} = 62.3$	
		$T_{iso} = 68.5$	

The principal value of the tensor **T** is largest along the symmetry axis ( $T_z > T_x = T_y$ ), while the principal axis of the tensor **g** is smallest along the symmetry axis ( $g_x = g_y > g_z$ ). This is typical for the SeO<sub>3</sub><sup>·</sup> radical [9, 10].

The large difference between the hyperfine parameters for radicals A<sub>1</sub> and A<sub>2</sub> is due to the presence of compensating ions in the vicinity of the radicals, which can change the distribution of unpaired electrons. For radical A<sub>1</sub> the oxygen O(1) is in the vicinity of the radical, while for A<sub>2</sub> it is far away from it. The radical disappears if either the oxygen O(1) again forms the bond Se–O(1) or drifts away from it, transforming into radical A<sub>2</sub>.

The temperature dependences of the principal values of the tensor **T** for radicals A<sub>1</sub> and A<sub>2</sub> are very different: they are temperature independent for A<sub>1</sub> and strongly temperature dependent for A<sub>2</sub> (figure 4). This can be explained in the following way. The radical A<sub>1</sub> with O(1) in almost its original position provides stability to this radical. A<sub>2</sub> with O(1) detached is more prone to thermal agitations, which leads to the temperature dependence of the components of the tensor **T**.

SeO<sub>3</sub><sup>·</sup> radicals A<sub>1</sub> and A<sub>2</sub> are very useful for studying the ferroelastic phase transition in KNSe. The large separation between the doublet lines, large anisotropy of the hyperfine constant and small linewidth allows one to study the phase transition very precisely. Radicals SeO<sub>4</sub><sup>·</sup> were not as useful due to an overlap of a few EPR lines and their small intensity.

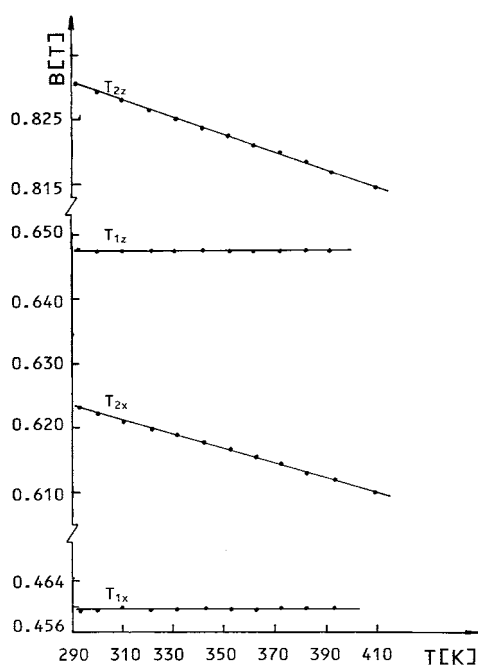


**Figure 4.** Temperature dependences of the principal  $z$ - and  $x$ -components of the tensor  $\mathbf{T}$  for radicals  $A_1$  and  $A_2$ .

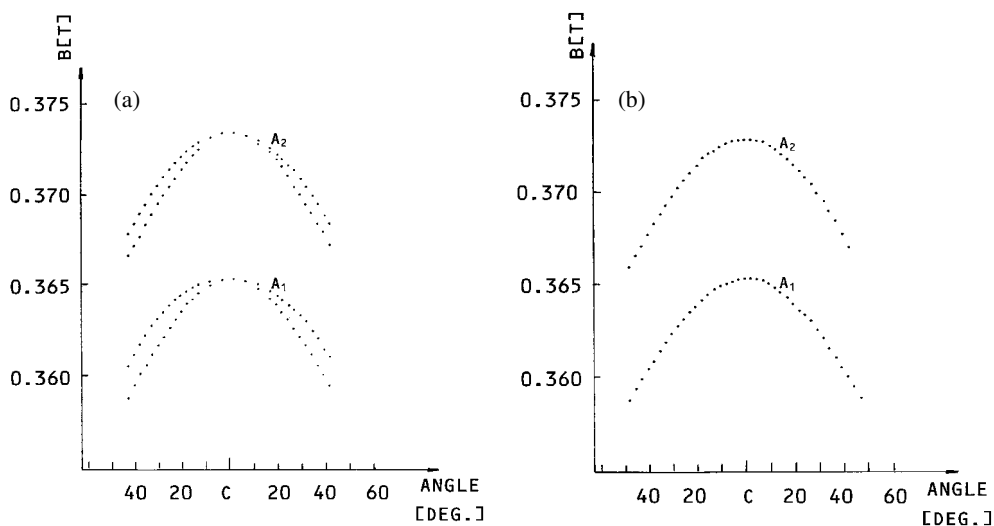


**Figure 5.** (a) An angular variation for centres  $A_1$  and  $A_2$  in the  $bc$ -plane at 293 K. The principal direction of the tensor  $\mathbf{A}$  is tilted  $3^\circ$  from the  $c$ -axis. (b) An angular variation for centres  $A_1$  and  $A_2$  in the  $bc$ -plane at 358 K. The principal direction of the tensor  $\mathbf{T}$  is along the  $c$ -axis.

There are two inequivalent radicals observed in the  $bc$ -plane (figure 3). The principal  $z$ -axis of the hyperfine tensor is deflected at room temperature by  $3^\circ$  from the  $c$ -axis, in the  $bc$ -plane (figure 5(a)). In the paraelastic phase the principal  $z$ -axis of the hyperfine tensor is

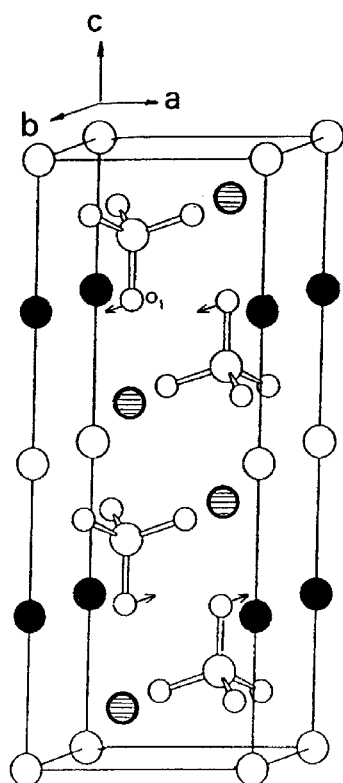


**Figure 6.** Two unit cells in the paraelastic phase with the tilt direction of the Se–O(1) bond indicated by small arrows. Se atoms are connected to oxygen atoms by double lines. Open circles indicate Na atoms, black circles K2 atoms and shaded circles K1 atoms. The figure was adapted from [6].

along the  $c$ -axis (figure 5(b)). According to x-ray diffraction results [6] the unit cell is doubled along the  $c$ -direction below  $T_c$ . Two unit cells of the paraelastic phase with the tilt direction indicated by small arrows are shown in figure 6. The  $3^\circ$  tilt angle in the  $bc$ -plane does not agree with the x-ray diffraction results, which show a tilt away from the  $bc$ -plane as well. This disagreement might be a reflection of the fact that the EPR technique probes the behaviour of the  $\text{SeO}_3^-$  radical, which is created by breaking the Se–O(1) bond in the  $\text{SeO}_4$  group. It is worth pointing out that x-ray diffraction in  $\text{KNCr}$  ( $T_c = 239$  K), which is isostructural with  $\text{KNSe}$  in both paraelastic and ferroelastic phases, showed that the tilt of the Cr–O(1) bond takes place in the  $bc$ -plane and it is approximately  $4^\circ$  at 230 K and increases to  $7^\circ$  at 200 K [11]. Similarly, x-ray diffraction results for  $\text{KNMo}$  crystal showed a large tilt of the Mo–O(1) bond in the  $bc$ -plane with only a tiny deflection from the  $bc$ -plane [1].

The angle between the Se–O(1) bond direction and the  $c$ -axis decreases gradually to zero when the crystal is heated and the phase transition is approached. Figures 7 and 8 show how the two inequivalent centres in the  $bc$ -plane coalesce into one in the heating run. Below the phase transition temperature  $T_c$ , two split lines are observed. When the temperature is increased the lines start to shift towards each other and then broaden. At about 329 K they coalesce into a single line, which narrows on further heating. This temperature dependence of the EPR lines can be explained by the gradual change of the orientation of the Se–O(1) bond relative to the  $c$ -axis. Above 329 K the Se–O(1) bond starts to fluctuate between two positions symmetrically

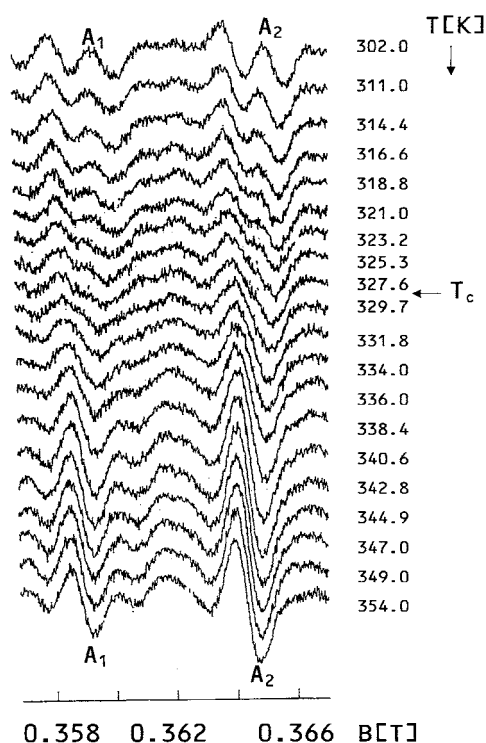


**Figure 7.** Temperature dependences of the high-field hyperfine curves for radicals  $A_1$  and  $A_2$  in the ferroelastic and paraelastic phases. Curves were recorded in the  $bc$ -plane,  $45^\circ$  from the  $c$ -axis, in the heating run. Two split lines coalesce into one at about 329 K and then get narrower with increasing peak-to-peak intensity.

located with respect to the  $c$ -axis. As the lines get closer and the rate of fluctuations becomes larger, the two lines coalesce into a single line. Well above  $T_c$  the frequency of the fluctuations is even higher, which leads to motional narrowing of the EPR lines. The phase transition in  $KNSe$  seems to be an example of crossover from displacive to order–disorder character. The only indication in EPR spectra of the existence of the ITP is the narrowing of the EPR lines and an increase of the peak-to-peak line intensity (figure 7).

It is quite striking that all macroscopic methods, such as the low-frequency dielectric, heat capacity, thermal expansion and birefringence ones, detect the phase transition at  $T_0 = 346$  K (an extremely small anomaly in the heat capacity was observed at  $T_c = 334$  K as well) [5]. High-frequency measurements, such as Raman scattering, Brillouin scattering and EPR ones, detect anomalies at about 334 K [7, 8].

Dynamical processes which at certain temperatures are static on the EPR measurement timescale might not be static when observed by a method using lower frequencies of measurements. This might explain the discrepancy between values of  $T_c$  detected by different techniques. It would be desirable to conduct measurements using the same technique but over a broad frequency range. It was suggested that librations of  $SeO_4$  groups about the threefold symmetry axis might be involved in the mechanism of the phase transition [7]. These librations, however, were associated with the phase transition at 334 K, while deviation of the  $Se-O(1)$  bond was associated with the phase transition at 346 K. The EPR measurements demonstrate that the lower phase transition is related to  $Se-O(1)$  bond deviation. If librations of  $SeO_4$



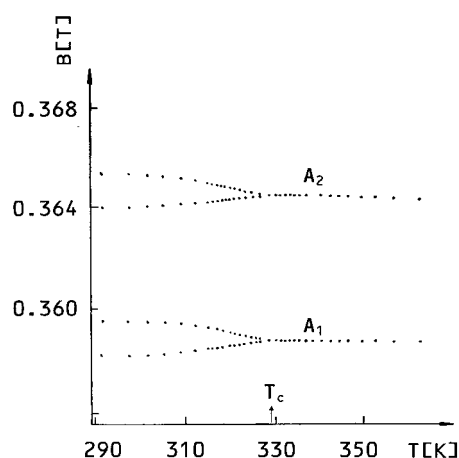


**Figure 8.** Temperature dependence of the line positions in the  $bc$ -plane, recorded at  $45^\circ$  from the  $c$ -axis, in the heating run. Two split lines shift towards each other. This corresponds to decrease of the tilt angle from the  $c$ -axis.

groups were related to phase transitions at 346 K, they would not be visible in the EPR spectra of the  $\text{SeO}_3^-$  radical due to its isotropic nature in the  $ab$ -plane.

The temperature  $T_c = 329$  K detected by the EPR method is lower than  $T_c = 334$  K previously reported. This could be due to the presence of defects created by  $\gamma$ -irradiation. In the cooling run the phase transition is observed at about 325, 5 K lower than in the heating run. This temperature hysteresis might explain the difference between  $T_c = 329$  and 334 K reported by different groups. It is also an evidence of the first-order character of the phase transition, although no sign of discontinuity of the EPR line splitting is observed.

#### 4. Conclusions

- (1) Irradiation of KNSe crystals by  $\gamma$ -rays produces  $\text{SeO}_3^-$  and  $\text{SeO}_4^{3-}$  radicals. The presence of two nonequivalent  $\text{SeO}_3^-$  radicals, designated as  $A_1$  and  $A_2$ , is explained in terms of their different associations with oxygen O(1), which provides charge compensation. One of the  $\text{SeO}_3^-$  radicals,  $A_2$ , is very stable even at elevated temperature.
- (2) The  $\text{SeO}_3^-$  radical is particularly useful for studying the phase transition in the KNSe crystal. Its orientation agrees perfectly with the orientation of the  $\text{SeO}_4^{2-}$  ion in the crystal lattice and faithfully represents changes occurring at the phase transition.
- (3) The mechanism of the phase transition is associated with ordering and tilt (displacement) of the Se–O(1) bond about the  $c$ -axis in the  $bc$ -plane. The ordering process is initiated at  $T_0 = 346$  K. Below  $T_c = 329$  K the direction of the Se–O(1) bond is gradually deflected from the  $c$ -axis in the  $bc$ -plane and reaches  $3^\circ$  at room temperature. Transformation from the paraelastic to ferroelastic phase is an example of the crossover from order–disorder to displacive character of the phase transition.
- (4) The existence of the temperature hysteresis of approximately 5 K (329 K in the heating run and 324 K in the cooling run) indicates a first-order phase transition at  $T_c$ .

#### Acknowledgment

SJ is very grateful to Professor J M Boggs, University of Toronto and The Hospital for Sick Children, for use of the EPR spectrometer in her laboratory.

## References

- [1] Fabry J, Petricek V, Vanek P and Cisarova I 1997 *Acta Crystallogr. B* **53** 596
- [2] Krajewski T, Piskunowicz P and Mroz B 1993 *Phys. Status Solidi a* **135** 557
- [3] Krajewski T, Mroz B, Piskunowicz P and Breczewski T 1990 *Ferroelectrics* **106** 225
- [4] Krajewski T, Piskunowicz P and Mroz B 1994 *Ferroelectrics* **159** 161
- [5] Diaz-Hernandez J, Manes J L, Tello M J, Lopez-Echarri A, Breczewski T and Ruiz-Larrea I 1996 *Phys. Rev. B* **53** 14 097
- [6] Fabry J, Breczewski T and Petricek V 1993 *Acta Crystallogr. B* **49** 826
- [7] Kaczmarzski M and Mroz B 1998 *Phys. Rev. B* **57** 13 589
- [8] Mroz B, Kiefte H, Clouter M J and Tuszynski J A 1992 *Phys. Rev. B* **46** 8717
- [9] Aiki K 1970 *J. Phys. Soc. Japan* **29** 379
- [10] Kawano T 1974 *J. Phys. Soc. Japan* **37** 848
- [11] Fabry J, Breczewski T and Madariaga G 1994 *Acta Crystallogr. B* **50** 13